Optimizing DNA Nanotechnology through Coarse-Grained Modeling: A Two-Footed DNA Walker

Thomas E. Ouldridge,[†,*] Rollo L. Hoare,[†] Ard A. Louis,[†] Jonathan P. K. Doye,[‡] Jonathan Bath,[§] and Andrew J. Turberfield[§]

[†]Department of Physics, Rudolph Peierls Centre for Theoretical Physics, [‡]Department of Chemistry, Physical & Theoretical Chemistry Laboratory, and [§]Department of Physics, Clarendon Laboratory, University of Oxford, Oxford OX1 3NP, United Kingdom

ABSTRACT DNA has enormous potential as a programmable material for creating artificial nanoscale structures and devices. For more complex systems, however, rational design and optimization can become difficult. We have recently proposed a coarse-grained model of DNA that captures the basic thermodynamic, structural, and mechanical changes associated with the fundamental process in much of DNA nanotechnology, the formation of duplexes from single strands. In this article, we demonstrate that the model can provide powerful insight into the operation of complex nanotechnological systems through a detailed investigation of a two-footed DNA walker that is designed to step along a reusable track, thereby offering the possibility of optimizing the design of such systems. We find that applying moderate tension to the track can have a large influence on the operation of the walker, providing a bias for stepping forward and helping the walker to recover from undesirable overstepped states. Further, we show that the process by which spent fuel detaches from the walker can have a significant impact on the rebinding of the walker to the track, strongly influencing walker efficiency and speed. Finally, using the results of the simulations, we propose a number of modifications to the walker to improve its operation.

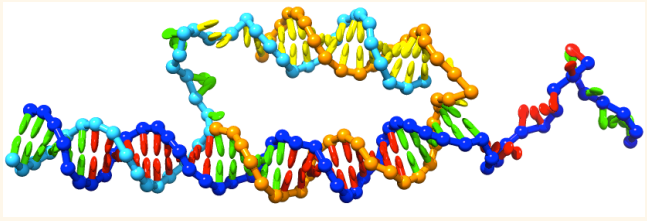

KEYWORDS: DNA nanotechnology · molecular motors · self-assembly · mesoscale modeling · simulation

The rapidly growing field of DNA nanotechnology offers the promise of controllable nanoscale engineering.[1] The potential utility of DNA arises from the same basic properties that allow the molecule to function as a repository of information for living organisms. Specifically, DNA consists of strands with a continuous sugar–phosphate backbone and bases (adenine A, thymine T, cytosine C, or guanine G) attached to the sugars.[2] Selective and anisotropic interactions between bases lead to the formation of structures such as antiparallel double-helical duplexes. Importantly, the interactions which stabilize the duplex are strongly dependent on base identity: to a first approximation, natural base pairing only occurs between complementary pairs A-T and G-C.[3]

This elegant Watson–Crick base pairing rule allows single strands of DNA to bind selectively to other strands when sequences are *complementary*. As a result, systems of single strands can be designed with sequences that lead to the self-assembly of complex structures[4] or the operation of dynamic machines.[5] For DNA nanotechnology to reach its full potential, however, optimization of design will be necessary. For example, a recent single-molecule study of a DNA walker[6] demonstrated incomplete assembly and operation of the device. The reasons for this behavior, which tends to reduce the efficiency of the walker, are not well understood.

Typically, DNA nanostructures and nanodevices are designed using well-established nearest-neighbor thermodynamic models of DNA duplex and single-stranded hairpin stability.[7] Unfortunately, these thermodynamic models cannot completely describe the operation of dynamic machines which are, by their nature, out of equilibrium and operate in a regime in which the kinetics of reactions are important. Similarly, the reaction pathways by which nanostructures form cannot be directly inferred from the overall thermodynamic changes associated

* Address correspondence to t.ouldridge1@physics.ox.ac.uk.

Received for review December 18, 2012 and accepted February 15, 2013.

Published online February 15, 2013
10.1021/nn3058483

with duplex formation. Nanodevices and nanostructures can also involve nontrivial multistranded complexes with pseudoknots[8] or complex internal loops whose stabilities have not yet been incorporated into thermodynamic models. In other cases, the three-dimensional structure of a DNA complex may result in tension or compression forces[9] that cannot be described without an explicit three-dimensional representation of the system.

Simulations of computational models of DNA have the potential to offer insight into the operation of nanodevices and the formation of nanostructures, as they can be designed to incorporate the kinetic, structural, and mechanical effects which are absent from the nearest-neighbor thermodynamic descriptions. Further, simply representing systems as realistic three-dimensional structures can be informative in its own right. To date, simulations have contributed very little to the field of DNA nanotechnology, as computational models were generally too slow or inaccurate to provide helpful information. Atomistic models using force fields such as AMBER[10] would be able to provide the most detailed information but would be prohibitively costly for large and complex systems. More coarse-grained approaches have the potential to access the relevant time scales, but models which provide a good description of the thermodynamical and mechanical changes associated with duplex formation have only recently been developed. This study demonstrates the utility of a recently proposed coarse-grained model[11] by using it to simulate the two-footed walker described in ref 12. We next discuss the operation of DNA nanodevices and walkers in more detail, before presenting simulations that explore the binding of the feet of the walker to its track.

DNA Nanodevices and Walkers. Two principles are central to many active DNA nanodevices.

- DNA binding can induce mechanical change, as binding causes strands to be held (quite rigidly) in close proximity, and unbinding causes this restriction to be released.
- A strand that forms an incomplete duplex with a substrate can be replaced by a strand with a greater degree of complementarity with the substrate.[13]

This process is known as *toehold-mediated strand displacement*. The potential for creating nanodevices using these principles was demonstrated by Yurke and co-workers who constructed "DNA tweezers"[14] that can be cycled between open and closed configurations through the sequential addition of two complementary strands. DNA hybridization and strand displacement have been used to create cages[15,16] that will open or close in the presence of specific ssDNA oligonucleotides. Strand displacement has also been applied to trigger the release of gold nanoparticles from within nanowires[17] and has been used to achieve topological rearrangement of large structures.[18]

It is possible to couple the mechanical changes of nanodevices to directional motion, resulting in "walkers" analogous to biological molecular motors. Typically, walkers have one or two feet that bind sequentially to consecutive sites on a track. The earliest designs required clocked addition of strands to generate coordinated, unidirectional motion[19,20] and were therefore not autonomous.

Autonomous, unidirectional motion must catalyze the release of free energy from a fuel source.[5] Walkers have been designed that assist in the catalysis of hydrolysis of the phosphodiester backbone of nucleic acids,[12,21−23] and an alternative source of free energy is in the catalysis of DNA hybridization itself.[24] Fuel strands, whose hybridization provides the free energy necessary to drive motion, can be designed to exist as metastable hairpins. By coordinating the cycle of a walker with the opening of these hairpins, the walker can be made to act as a catalyst for fuel hybridization.[25,26] Many autonomous walkers generate unidirectional motion through modification of the track.[21−23,25] By coordinating the interaction of the feet of a two-footed walker with its track, the possibility of autonomous motion on a track that can be reused has also been demonstrated.[12,26]

References 12, 19−23, 25, and 26 use toehold-mediated strand displacement to effect conformational change. Walkers have also been designed based on the migration of a four-armed (Holliday) junction.[27,28] The principle is very similar: instead of one strand displacing another, base pairs are transferred between helices at the branch point.

Artificial walking devices present a number of possible applications. For example, such machines have the potential to function as active agents in a molecular assembly line. Preliminary studies have shown the possibility of using DNA hybridization to accelerate chemical reactions by bringing reagents into close proximity[29] and the possibility of using a walker to selectively pick up gold nanoparticle cargo.[30]

Most of these systems have been studied using ensemble measurement techniques such as bulk fluorescence spectroscopy[12,20,21,26,27] and gel electrophoresis.[12,19,20,22,25−28] Such measurements can demonstrate biased movement but often provide only limited information on the stepping process. Recent single-molecule studies, using techniques such as single-molecule FRET[6] and real-time atomic force microscopy,[23] provide more information on walker mechanisms. We expect that the current study will inspire a new generation of single-molecule experiments that are informed by coarse-grained simulation and that allow all aspects of the designed operating cycle to be tested and optimized.

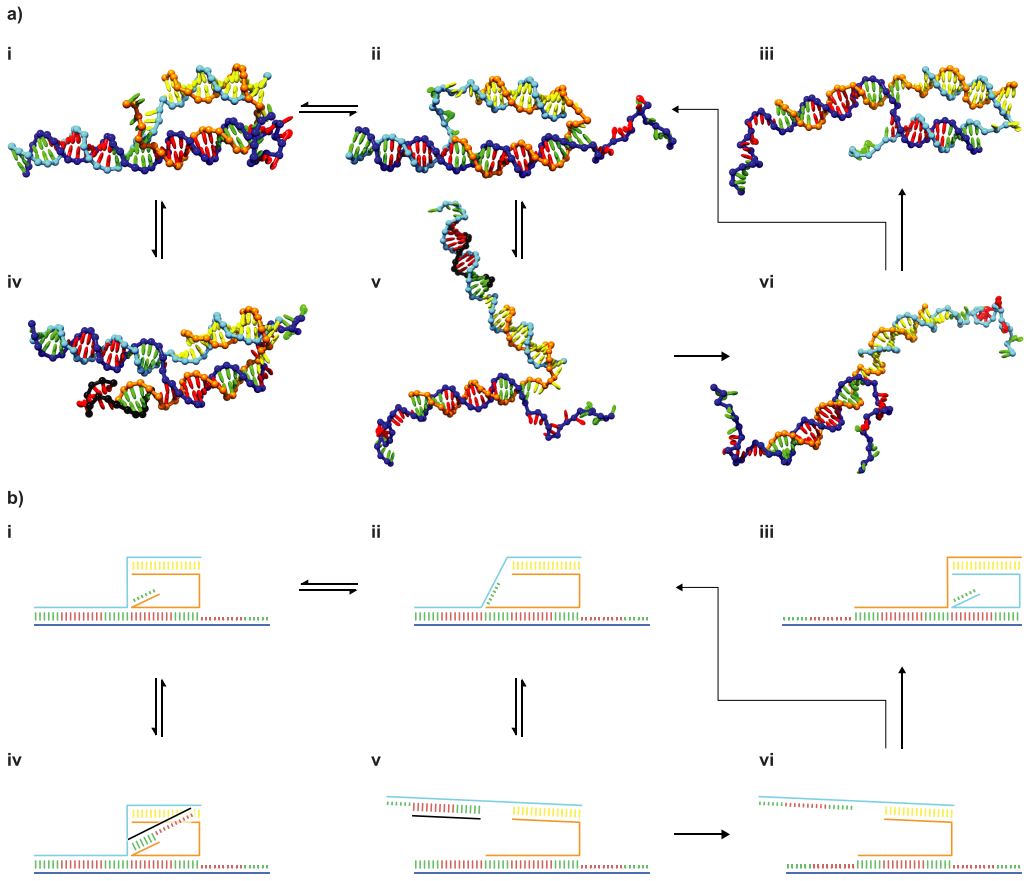

Figure 1. The walker and its operating cycle on a three-site track, as represented by the coarse-grained model (a), with accompanying schematic illustrations (b). In all images of the walker, the *backbone* of the track is colored dark blue, the stationary foot orange, and the second foot sky blue. The backbone of the fuel is colored black. *Bases* are colored to represent the domains defined in Table 1. The "competition" domains (where binding sites overlap) are green, the "binding" domains are red, and the other bases in the body of the walker are yellow. Initially, the walker is in equilibrium between states (i) and (ii), with front or back competition domains exposed. Fuel can bind to either raised competition domain ((iv) and (v)) but can only progress with displacement in the case of binding to the back foot (v). Once bound to the foot, the fuel can be cleaved by the nicking enzyme. Once cleaved, the fuel-foot duplex is unstable. State (vi) shows the walker with a raised foot after the fuel has detached: the foot can then reattach to the track either behind (an idle step returning to state (ii)) or in front of (a forwards step to state (iii)) the stationary foot. Double arrows indicate steps for which the free-energy change is expected to be marginal, whereas single-arrow transitions indicate those for which there is a significant decrease in free energy, resulting in irreversibility under walker operating conditions.

RESULTS AND DISCUSSION

System and Model. *Two-Footed DNA Walker.* In this work, we study the operation of the two-footed DNA walker proposed by Bath *et al.*[12] and illustrated in Figure 1. The relevant DNA sequences are given in Table 1. The walker has two identical single-stranded "feet" that are connected by a duplex. The feet are designed to hybridize to adjacent sites on a single-stranded track. As neighboring binding sites partially overlap, adjacent feet compete for binding to the track through competition domains that are present at both ends of either foot. Base pairs between foot and track that are not part of the competition domains constitute "binding" domains. When single-stranded (*i.e.*, out-competed for binding to the track), either competition domain can bind to a fuel strand that is also present in solution.

If the fuel binds to the competition domain of the back foot, then it is also able to displace the track from the rest of the foot *via* a conventional strand displacement reaction, thereby "raising" the foot (we define the terms *back* or *backward* as in the direction of the 5′ end of the track and *front* or *forward* by the direction of the 3′ end of the track). If, however, the fuel hybridizes to the front-foot competition domain, the strands are not correctly oriented for branch migration and displacement cannot occur directly. In this case, the fuel should detach without raising the foot. The walker is therefore designed to raise preferentially the back foot.

A recognition site for N.BbvC IB, a nicking enzyme,[31] is present in the fuel (the sequence in question is CC*TCAGC—the asterisk indicates the nicking location). The enzyme can cleave the fuel but only when it forms part of a duplex (the duplex partner is not cleaved). The enzyme will therefore tend to cut the fuel when it is bound to a raised foot—the nicking site is absent in the foot/track duplexes due to the presence

TABLE 1. Sequences Used for the DNA Walker[a]

Strand	Sequence
Track (2 sites)	5′- AGCATC CÎTCAGCÎTC AGCATC CÎTCAGCÎTC AGCATC -3′
Walker 1	5′- GTATTATCGTTAGTCT tttt GATGCT GAĜGCTGAĜG GATGCT -3′
Walker 2	5′- AGACTAACGATAATAC tttt GATGCT GAĜGCTGAĜG GATGCT -3′
Fuel	5′- CCTCAGCC*TC AGCATC -3′

[a] Complementary regions are highlighted in the same color (corresponding to the colors used for the bases in Figure 1). The competition domains are highlighted in green and the binding domains in red. Other bases in the body of the walker are highlighted in yellow. Circumflexes indicate mismatched bases between the foot and track (which prevent the track from being cleaved, and also favor foot-lifting by the fuel), and the asterisk indicates the cleavage site within the fuel that is cut by the nicking enzyme. The track can be extended by adding additional binding and competition domains.

of designed mismatches, preventing cleavage of the track. The cut fuel/foot duplex is unstable and will eventually dissociate, allowing the foot to rehybridize to the track. If rebinding occurs in front of the other foot, the walker has stepped forward; otherwise, the system returns to its original state in an idle step.

As a result of the asymmetry of lifting the feet, the walker undergoes unidirectional, autonomous motion. This is possible because the motion of the walker is coupled to enzymatic cleavage of ssDNA fuel strands, giving it the potential to perform work. It is important to emphasize that the mechanism for preferential lifting of the back foot is dependent on the feet being bound to adjacent sites on the track, and that the absence of a foot replacement bias would limit the walker to 50% efficiency. In this work, we will explore the possibility of creating a foot replacement bias and whether the feet will indeed bind only to adjacent sites on the track.

To date, the principle of operation of the walker has been demonstrated on a short track of two sites.[12] Preferential lifting of the front foot by a fuel strand has been achieved (as has lifting of the back foot by a "reverse fuel"). The release of the fuel has also been shown, and walkers have been found to successfully catalyze the hydrolysis of ≥64 fuel strands. The kinetics of rebinding to the track after nicking of the fuel by the enzyme, which is the subject of this work, cannot be reliably inferred from the available experimental data. A similar hybridization-driven walker has also been demonstrated on a three-site track.[26]

Coarse-Grained Model of DNA. Coarse-grained models cannot hope to recreate accurately all properties of DNA. It is therefore important to use a model which captures the properties most relevant to walker operation. We use the model of Ouldridge *et al.*,[11,32] which was designed to give a good representation of the average structural, mechanical, and thermodynamic properties of single- and double-stranded DNA and has the potential to explore non-equilibrium processes. Capturing such features is important in modeling the walker, which contains single-stranded and duplex components, adopts nontrivial structures involving complex loops, and relies upon hybridization

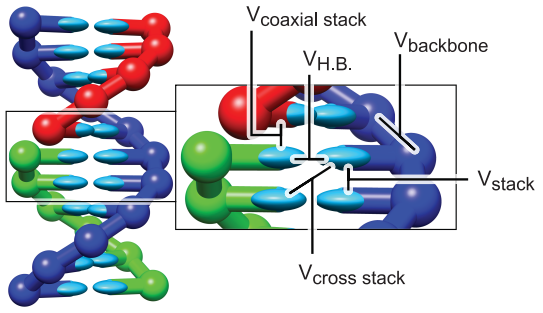

Figure 2. Model DNA, with stabilizing interactions indicated. The backbone sites are shown as spheres, the bases as ellipsoids. All nucleotides also interact through short-ranged repulsive excluded volume interactions.

reactions including strand displacement. The model was first used to study the operation of DNA nanotweezers.[33] An improved version was discussed in detail in ref 11, and the version used in this work (which includes coaxial stacking) is given in ref 32. The robustness of the model has been confirmed by the study of a number of systems and phenomena that were not considered in its parametrization: duplex overstretching under force,[34] cruciform formation under applied torsion,[35] the formation of a liquid crystal at high density,[36] and strand displacement as a function of toehold length have all been successfully modeled.

The potentials which constitute the coarse-grained model are given in detail in refs 11 and 32. Model DNA consists of a string of nucleotides, each represented by a rigid body with one interaction site for the backbone and two for the base. Figure 2 shows the model's representation of a short double-helix. The potential energy of the system can be decomposed as

$$V = \sum_{\langle ij \rangle} (V_{\mathrm{bb}} + V_{\mathrm{stack}} + V_{\mathrm{exc}}') + \sum_{i,j \notin \langle ij \rangle} (V_{\mathrm{HB}} + V_{\mathrm{cr.st.}} + V_{\mathrm{exc}} + V_{\mathrm{cx.st.}}) \quad (1)$$

in which the first sum runs over all pairs of adjacent nucleotides on the same strand and the second sum includes all other pairs. The interactions are all short-ranged, meaning that only a small fraction of possible interactions need to be calculated at each step, thereby making the model more computationally efficient.

The interactions relevant to the duplex state are shown in Figure 2. The backbone potential V_{bb} acts as an isotropic spring, limiting the distance between backbone sites of neighbors and mimicking backbone connectivity in a strand. The hydrogen bonding (V_{HB}), cross stacking ($V_{cr.st.}$), coaxial stacking ($V_{cx.st.}$), and stacking interactions (V_{stack}) explicitly depend on the relative orientations of the nucleotides as well as the distance between the relevant interaction sites. The orientational dependence reflects the fact that bases are highly asymmetric and ensures that a right-handed, antiparallel helical duplex is the lowest energy state for two complementary strands. For simplicity, model helices are symmetrical rather than having asymmetric major and minor grooves, and all four nucleotides have the same size and shape. Bases and backbones also have excluded volume interactions V_{exc} or V_{exc}' to represent the space occupied by nucleotides. Finally, the coaxial stacking term represents stacking interactions between nearby bases that are not directly connected to each other by the sugar–phosphate backbone.

The sequence specificity of Watson–Crick base pairing is ensured by only including hydrogen-bonding interactions between complementary pairs of bases AT and CG. No other sequence dependence is included in the model. Consequently, the model parameters were fitted to reproduce melting temperatures of average oligonucleotides in SantaLucia's nearest-neighbor model[37] and the average structural and mechanical properties of double- and single-stranded DNA. The model was fitted to experiments performed at a high monovalent salt concentration $[Na^+] = 0.5$ M, where the strength of screening makes the representation of electrostatic repulsion through short-ranged excluded volume interactions reasonable.

We have directly simulated all stages of walker operation shown in Figure 1, with the necessary exception of enzymatic cleavage. The most interesting results relate to the binding of feet to the track (from state (vi) to state (ii) or (iii) in Figure 1), and these findings are reported here. We first consider the binding to a short track (consisting of three sites) with and without tension applied to the track. We then extend our study to include longer tracks. We consider the system exactly as introduced by Bath *et al.*[12] at a temperature of 310 K. In the design,[12] it is implicitly assumed that complete fuel dissociation occurs before foot rebinding. This may not be true, however. For clarity, we initially present results for rebinding in which there is no fuel present, as these are simpler to analyze and understand; the possible influence of fuel fragments is explored later. Throughout this work, we will consider one foot to be permanently in place on the track. This will be known as the *stationary foot*. We will also use the terms *correct* or *intended* base pairs to refer to those base pairs between track and foot which are anticipated to form in the design; *misbonds* or *unintended* base pairs are interactions between the strands which were not anticipated in the original design.

Foot Rebinding on a Short Track. *No Applied Tension.* In order to study the reattachment of the foot to the track, 50 independent kinetic simulations were performed on a walker with one foot attached to the center of a three-site track. The other foot was initially raised with the possibility of binding in front of or behind the stationary foot. These simulations can be used to study the propensity of the system to take an idle or a forward step (corresponding to moving from state (vi) to state (ii) or (iii), respectively, in Figure 1). Simulations were run for 5×10^9 integration steps, corresponding to a nominal time of 26 μs (simulation time scales are discussed in more detail in the Supporting Information). It should be noted that absolute times in coarse-grained models are less reliable than relative rates for similar processes,[44] and we will focus on the latter here. The states of the systems at the ends of simulations are reported in Figure 3a. In the majority of cases, the initially raised foot bound to the track during simulation. In some cases, it directly formed the intended base pairs with either the front or back site of the track. In other cases, metastable misbonds formed instead, typically involving around six base pairs. A common misbond motif is shown in Figure 3d; this structure involves seven base pairs enclosing one internal mismatch. The misbonds were sufficiently stable that many survived until the end of the simulations. In some simulations, however, the misbonds melted (the foot spontaneously detached from the track), allowing reattachment in another configuration. In others, internal rearrangement allowed misbonds to be replaced by correct binding between track and foot without the foot first detaching from the track. The details of internal displacement mechanisms are the subject of a forthcoming publication. Given enough simulation time, all systems would eventually bind correctly to either the front or back site.

The walker was not intentionally designed to have a bias associated with foot replacement, and on an extended track, the energies after forward and idling steps are identical. Figure 1 (vi), however, clearly illustrates a geometric asymmetry in the walker: the raised foot is attached to the front end of the stationary foot. Using such an asymmetry to generate a kinetic bias for foot replacement would be extremely beneficial as, without it, the walker's efficiency is limited to 50%. The evidence from our kinetic simulations is that the geometrical asymmetry does not manifest itself as a bias toward stepping forward correctly, although there is a clear bias for misbonding with the front site rather than the back site. As shown in Figure 3a, the numbers of simulations that ended with the walker bound correctly to either the front or back site were

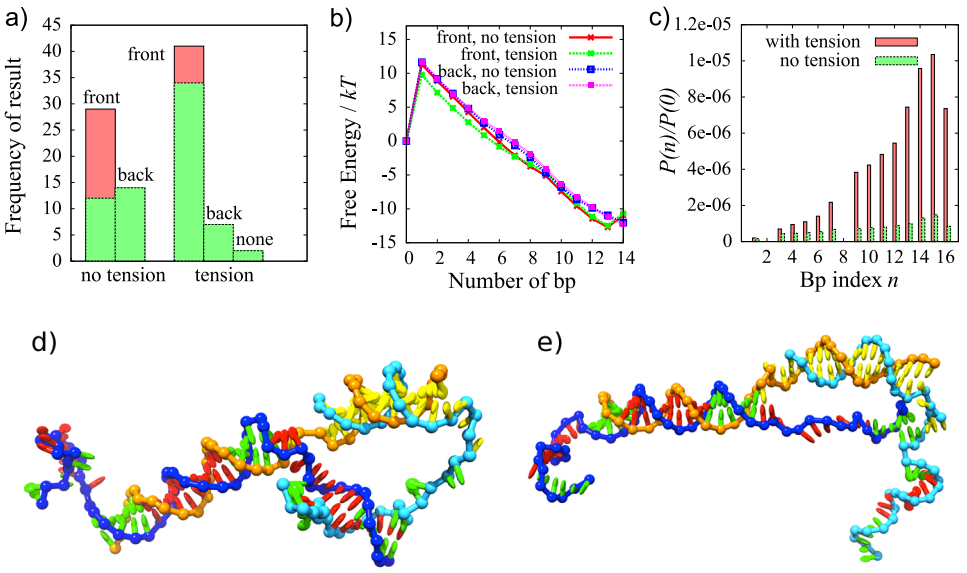

Figure 3. Results of foot attachment simulations for short tracks. (a) Final state of 50 kinetic simulations initiated with one foot in the raised state, both with and without a tension of 14.6 pN applied to the track. The height of a column indicates the total number of simulations that ended with bonding to the relevant site: this is subdivided into green (correct bonding) and red (misbonding). (b) Free-energy profile of bonding to the front and back sites as a function of the number of correct base pairs (bp), measured relative to the state with no bonds, for systems with and without tension. (c) Equilibrium probability $P(n)$ of being in a state with a single base pair between the foot and the front site of the track as a function of the position of that base pair within the site (n), normalized by the equilibrium probability of having no base pairs between track and foot ($P(0)$). Here position $n = 1$ is immediately adjacent to the stationary foot, and $n = 16$ is at the front end of the track. Results are shown for simulations with and without a tension of 14.6 pN applied to the track. The gaps at 2 and 8 arise from the mismatches designed into the foot/track duplex to avoid enzymatic cleavage of the track. (d) Example of a typical misbonded configuration, in which the foot has bound to the front site in an unanticipated way. (e) Example of a state involving a single base pair contact between foot and track at the front end of the track. Note the stretching of ssDNA along the length of the walker's body.

approximately the same. Even if all the misbonds would eventually have resolved into correct binding with the front site, this would still leave a ratio of only ~2:1 in favor of stepping forward.

The lack of bias is initially surprising because in Figure 1 (vi) the raised foot appears to be naturally closer to the front site. However, in order to form a correct base pair between the foot and the front site of the track, single-stranded sections of foot and/or track must stretch along the length of the 16 bp (base pair) duplex bridge that forms the body of the walker and links the two feet together. For example, the base that is designed to bind to the base at the front end of the track is close to the body of the walker. For these bases to hybridize as designed, the track must extend all the way along the walker's body to meet the corresponding base in the foot, as is illustrated in Figure 3e. Similar extension is needed for all other pairs. As ssDNA has a very short persistence length,[45] such extension is rare. Forming correct base pairs with the back site, by contrast, does not require stretching of ssDNA, only approximate anti-alignment of the walker body and the stationary foot.

To further investigate the lack of bias, we measured the free-energy profile of bonding to the front and back sites as functions of the number of correct base pairs. Thermodynamic simulations were performed, using umbrella sampling to enhance equilibration. Details of the simulations are provided in the Supporting Information. As is evident from the profiles without tension in Figure 3b, the free-energy cost of forming the first few base pairs is essentially identical in both cases, which reflects the fact that the difficulty of forming intended base pairs with either site is comparable.

Track under Tension. We have argued that walker asymmetry does not result in a large bias for rebinding to the front site due to the difficulty of stretching ssDNA over the length of the duplex body of the walker. A possible method for eliminating this difficulty would be to apply a tension to the track. The operation of the walker on a stretched track is also worth considering in of itself, as tracks will need to be held under tension if they are to provide a short route between two specific locations for the walker. Further, it might be expected that stretched tracks help to prevent binding of the walker's feet to nonadjacent sites, a possible complication in walker operation that we will explore later.

Figure 3a shows the result of simulations identical to those described in the previous section except for the application of a tension of 14.6 pN to the track. A force of this size is reasonable for DNA-based systems: it is comparable to the tension required to unzip typical hairpins at 0.5 mM [Na^+][46] but much smaller than the longitudinal force necessary to disrupt duplexes at room temperature.[47] As hairpins unzip at around

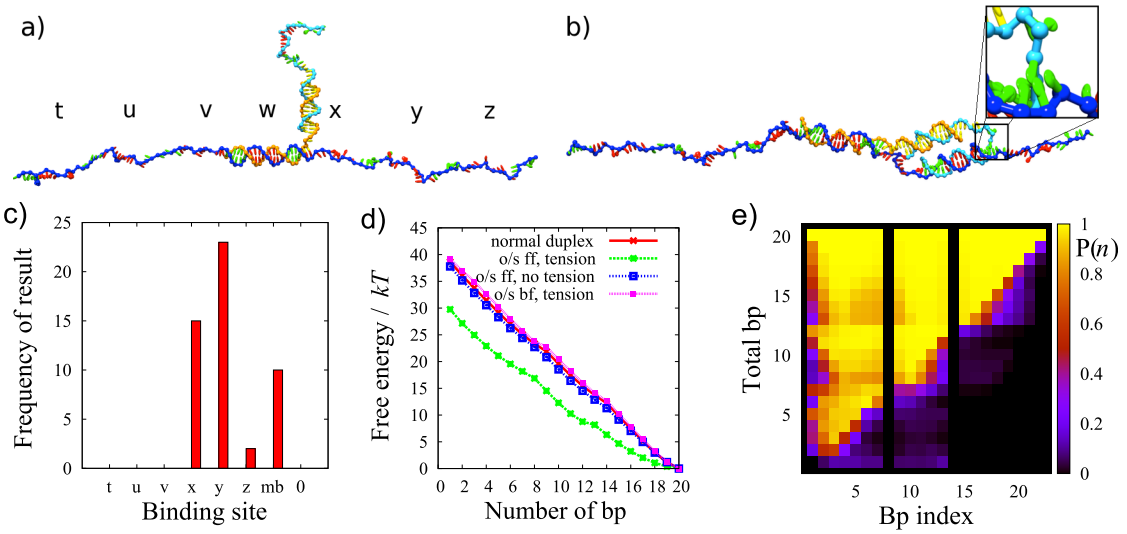

Figure 4. Results of foot attachment simulations for long tracks under 14.6 pN of tension. (a) Snapshot of a walker on a five-site track with a raised foot, indicating the labeling of binding sites. (b) Walker bound to sites *w* and *y* (a single overstep). This snapshot shows a state in which three bases have frayed from the front of the foot/track duplex, a process which is favored by tension. This fraying is highlighted in the inset. (c) Final states obtained from 50 kinetic simulations, showing the binding site (states recorded as "0" had no binding at the end of the simulation, and "mb" implies a misbond, the majority of which were with sites *x* and *y*). (d) Free-energy profile of fraying for track/foot duplexes in various environments. The "normal duplex" considers the foot/track system in isolation, without the rest of the walker. Other simulations explicitly included the whole walker: all were sampled in the overstepped (o/s) state, with the front foot bound to site *y* and the back foot to site *w*. The profiles were obtained for the front foot (ff) with and without 14.6 pN of tension and for the back foot (bf) with the track under tension. (e) Map of the probability that a base pair is present between the foot and track site *y*, as a function of the total number of base pairs and the position of the base pair in question within the track (index "1" corresponds to the rearmost base pair and "22" the foremost). The tendency of the duplex to fray from its front edge is clear. The black stripes at indices "8" and "15" arise from the mismatches designed into the track/foot duplex to prevent cleavage of the track.

14−19 pN,[46] a long A-T rich hairpin sequence could be added to the end of an extended track to act as a force clamp to maintain a tension of around 15 pN.

Our simulation results in Figure 3a indicate a significant (though not overwhelming) bias for stepping forward. This bias is largely due to an increased rate of binding directly to the front site, as the tension holds the forwardmost bases in a more accessible location. Figure 3b shows that the free energetic cost of forming the first few base pairs with the front site is now significantly lower than without tension and lower than the cost for binding to the back site by around $1.9k_BT$. Further clarification follows from Figure 3c, which shows the equilibrium probability of a single correct base pair existing between the foot and front site as a function of its position on the track. Binding to the bases at the very front of the front site is far more favorable under tension. The findings are not particularly sensitive to the precise value of the tension: shorter simulations using a tension of 7.3 pN produced qualitatively similar results.

It is also interesting to note that the fully bound complexes are barely affected by a tension of 14.6 pN, as can be seen by comparing the free-energy profiles with and without tension in Figure 3a for high numbers of bonds. If the system were in equilibrium, the approximately equal free energies for full binding in front of or behind the fixed foot (which would be strictly equal in the limit of a long track) would imply faster detachment from the front site to compensate for faster attachment. In operation, however, the walker is kept out of equilibrium, and the dominant transition states for raising a foot (which involve binding of the fuel, as the free-energy barrier for unassisted detachment of a foot from the track is very large) are totally different from those for attachment. Rates of foot-lifting are therefore likely to be determined by the rate at which the fuel can displace the track from the feet and hence are likely to be relatively unaffected by this tension. Consequently, the DNA model suggests that applying a moderate tension could result in a bias for placing a raised foot down in front of an attached foot without reducing the known bias associated with foot-lifting. This behavior results from the fundamentally non-equilibrium nature of the walker's operation, highlighting the utility of the coarse-grained model for analysis of such a system.

Foot Rebinding on a Long Track. To perform any useful task, the walker will have to take consecutive steps along an extended track with many binding sites. To date, such a system has not been studied experimentally. We have explored the feasibility of walker operation on an extended track by simulating seven binding sites (hereafter labeled *t*-*z* from back to front) illustrated in Figure 4a, with one foot of the walker initially bound to the central site *w* and the other raised. Here we report only results from simulations in which the track was subject to 14.6 pN of tension. Simulations

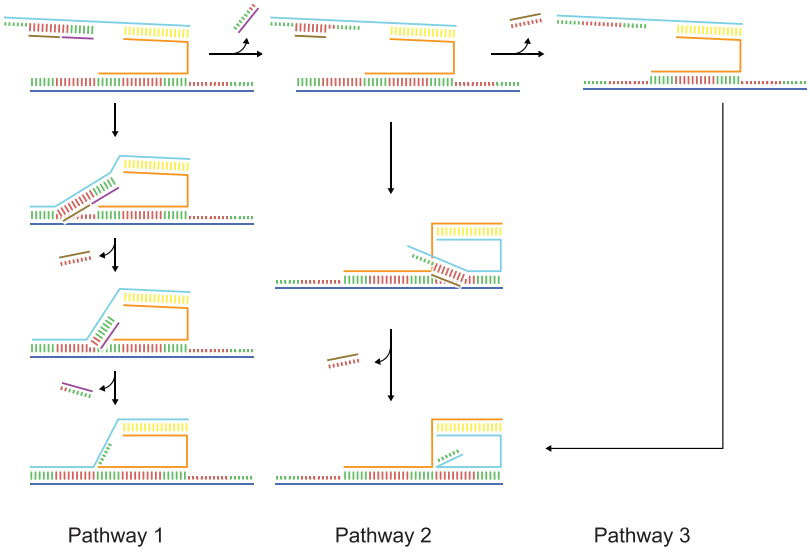

Figure 5. Possible processes that could lead to foot rebinding. Pathway 1 shows the foot rebinding to the track by the available competition domain after the fuel has been cut, with the fuel halves then being displaced by the track. Pathway 2 shows the foot rebinding after the proximal half of the fuel has already detached, with the track then displacing the remaining distal half. A similar process could occur with the distal half detaching first. Pathway 3 shows rebinding only after all of the fuel has detached, corresponding to the case considered in the earlier stages of this work. These diagrams neglect any effect of possible continued binding of the nicking enzyme.

were performed for 3.5×10^9 integration steps (a nominal 18 μs), and the states of the system at the end of each simulation are reported in Figure 4c.

The most common result is binding to site *y*, a single "overstep" in the forward direction. Such a state is illustrated in Figure 4b. It is even possible to double overstep, resulting in binding to site *z*. Overall, there is a large bias for binding in front of the attached foot (to site *x*, *y*, or z) rather than behind it (to *t*, *u*, or *v*). In fact, no binding to the three back sites was observed in these 50 simulations. Unfortunately, overstepping is not an advantageous outcome: the mechanism of selective lifting of the back foot by the fuel relies upon the two feet being bound to adjacent sites on the track, to prevent one competition domain from being bound and make it available for fuel binding. At first glance, an overstepped walker appears to be stuck—a rare event is required to lift one foot or the other (possibly blunt-ended strand displacement by the fuel). These results are not overly sensitive to the precise value of the tension: reducing it to 7.3 pN produces qualitatively similar results, with the main difference being that more walkers are more likely to bind to site *z* due to the reduced extension of the track.

Overstepping under tension is not, however, as disastrous as it seems. For the foot to fully bind to sites *y* or *z*, the walker must stretch further than usual or the track must reduce its extension. Both cost free energy and, as a result, the overstepped foot/track duplex tends to fray (lose base pairs) from its forward edge more than when binding to site *x*. An overstepped walker state exhibiting some degree of fraying is shown in Figure 4b. We performed thermodynamic simulations of the free-energy profile of bonding to quantify this fraying (details are provided in the Supporting Information). Identical simulations were performed for a walker bound to sites *w* and *y* in the absence of tension on the track and for an isolated duplex with the same sequence as the foot/track duplex. The results, shown in Figure 4d, indicate that the foot/site *y* duplex frays far more than an isolated duplex when the track is under tension but behaves like an isolated duplex in the absence of tension. Furthermore, when the front foot of the walker is bound to site *y*, the back foot on site *w* does not show increased fraying under tension (due to the asymmetry of the walker, fraying of the back foot does not significantly reduce the tension in the system). Figure 4e, which shows the prevalence of certain base pairs as a function of the total number in the foot/track duplex, indicates preferential fraying from the front end of the foot/track duplex. Fraying is even more pronounced for a double-overstepped walker bound to site *w* and site *z*.

Fraying of the front foot/track duplex from its forward edge reveals a toehold for fuel binding. Track tension will also make displacement an easier process once it has started, as the walker/track base pairs are less stable in an unstrained foot/fuel duplex. As a result, recovery from the overstepped state will be easier than might naïvely be expected when the track is subjected to tension, but the tendency to overstep will still reduce the efficiency and speed of operation of the walker significantly.

Effect of Fuel Fragments. In the original design of the walker, and in the discussion presented so far, it is

assumed that the binding of a foot to the track occurs only after the severed fuel and nicking enzyme have completely detached from the foot, and hence that the fuel and enzyme play no role in the reattachment. It is not obvious, however, that this conjecture is true. We can imagine the following alternatives.

- The track displaces both halves of the nicked fuel before the fuel detaches spontaneously.
- The track displaces one-half of the fuel after the other half has spontaneously detached from the raised foot.

The dissociation of the nicking enzyme is an additional complication that we will not consider further. Examples of these alternative mechanisms are illustrated in Figure 5, as pathways 1 and 2. Pathway 3 shows the route that has been assumed thus far. Pathway 1 would be extremely disadvantageous, as the domain of site *x* that could function as a toehold for this displacement by the forward site is sequestered by the stationary foot. The same is not true of other sites, however, so pathway 1 would tend to favor overstepping or an idle step. The consequences of the pathway 2 are less obvious.

Rebinding to a Track under Tension before Any Fuel Has Detached. In this section, we estimate the probability that the foot rebinding occurs before any of the fuel has detached spontaneously. We wish to compare the rate at which nicked fuel spontaneously detaches from a raised foot to the rate at which it detaches due to displacement by the track. Both are slow processes, and direct simulation proved to be impractical. We therefore used forward flux sampling to estimate the rates of spontaneous fuel dissociation and displacement of the distal half of the fuel by site *v*; more details are given in the Supporting Information. Due to the presence of the stationary foot, the track cannot directly displace the whole of the proximal half of the fuel (the half closest to the walker body): at least six base pairs must melt spontaneously. However, it is much more probable that this will occur than that foot will spontaneously dissociate from the track (breaking 12 base pairs), so we take successful displacement of the distal half of the fuel as a proxy for successful binding to site *v*.

Our forward flux sampling simulations suggest that spontaneous dissociation of both proximal and distal fuel fragments is ~8 times slower than displacement of the distal fragment by site *v* in our model: spontaneous dissociation of either half is ~4 times as slow. Although the precise branching ratio of these pathways depends on details such as the destabilizing effect of mismatches between track and foot (which is known to be somewhat underestimated in the model[11]), the model suggests that the first stage of fuel displacement is likely to occur both by spontaneous dissociation and displacement by the track with reasonable

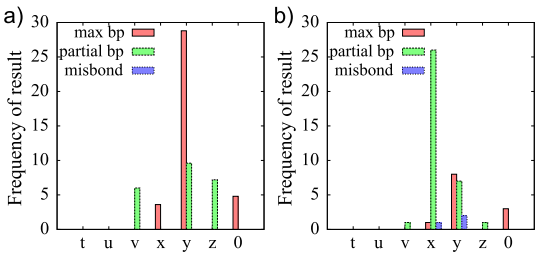

Figure 6. Results of 50 kinetic simulations each for rebinding of a foot to an extended track under 14.6 pN of tension, with (a) proximal and (b) distal half of the fuel still remaining. The graphs show the number of simulations for which binding to each site was observed. Correct attachment to part of the binding site (without fully displacing the fuel remnant) is recorded as "partial bp", and full binding (having displaced the fuel) is "max bp"; "0" indicates that simulations ended with the foot unattached to the track. In no simulations was the fuel observed to detach without displacement by the track.

frequency. As displacement before dissociation of the fuel disfavors binding to the intended site *x*, which has no toehold to initiate the displacement, any optimization of the walker should consider limiting the effectiveness of the displacement pathway. We also note that site *y* on an extended track has a toehold that facilitates displacement of the proximal half of the fuel before any spontaneous dissociation has occurred, leading to an overstep. This possibility, however, can be eliminated more easily than for site *v* by changing the design of the track, as outlined in the discussion.

Rebinding to a Track under Tension by Displacing Half of the Fuel. Having studied the possibility of rebinding without any spontaneous fuel detachment, we now consider systems in which half of the fuel has detached. We perform simulations identical to those for binding of a foot to a long track under tension but this time initialize systems with either the distal or proximal halves of the fuel still attached. Fifty kinetic simulations of 3.5×10^9 steps were run for each case. The final states of the systems in the simulations are given in Figure 6.

The first thing to note is that attachment to the track occurs much faster than the dissociation of the second half of the fuel, suggesting that the fuel remnant will have a large role to play in the kinetics of rebinding. Once again, misbonded states are possible.

If the proximal half of the fuel remains, binding to the intended site *x* is strongly inhibited (although possible) as the most favorable bases for forming the first contact (the competition domain closest to the walker's body) are covered by the fuel. Most systems bind to site site *y* and some to site *v*, both of which have 12 contiguous base pairs available even with the fuel fragment in place. In all cases, displacement of the fuel is then hampered by the need to enclose a mismatch in the foot/track duplex. Further, the front end of site *v* is sequestered by the stationary foot, inhibiting displacement. As a result, complete displacement of the fuel

fragment by site *y* (once the foot is bound) is slow, and complete binding to site *v* requires the spontaneous breaking of at least six base pairs between fuel and foot before the fuel detaches. Displacement by site *y* is also hampered by the destabilization of the front foot/site *y* by tension that was discussed earlier. Nonetheless, detachment of the fuel is expected to occur faster than the melting of the longer foot/track duplex in the case of *y* and *v* binding, and so we expect that systems which were found partially bound to *y* and *v* would eventually become fully bound if simulated for longer.

If the distal half of the fuel remains, no site has more than eight contiguous base pairs available. The most common behavior involves binding to bases at the front of site *x* or the back and front of site *y*. The relative lack of binding to site *v* reflects the tension-induced bias observed for the fuel-free system in Figure 3, which is exacerbated by the presence of the distal fuel fragment. Once again, displacement of the fuel fragment is slow due to the mismatches between foot and track, but the eight possible base pairs with the front of site *x* are sufficiently strong that partially bound tracks are expected to displace the fuel fragment eventually (such an event was observed in one simulation).

The consequences of the presence of a single fuel remnant are thus strongly dependent on which half remains. If the proximal half of the fuel remains, binding to the intended site *x* is suppressed and overstepping to site *y* or an idle step to site *v* is more common. If the distal half remains, however, the tension-induced bias for stepping to site *x* rather than *v* is maintained and overstepping is not dominant.

As shown in Figure 6, the formation of misbonds with the track is also possible while the fuel is still bound to the foot. These misbonded structures cannot directly displace the fuel from the foot and are less stable than the fuel/foot duplex. In general, they are expected either to eventually melt or to be internally displaced by correct binding to the track (both of which have been observed in simulation). In the first case, once the misbond has melted, the system returns to the initial state of the system. In the second case, internal displacement favors base pairs that have not been sequestered by the fuel, which are exactly the base pairs that tend to form in the absence of misbonds. Misbonding does not, therefore, qualitatively affect this analysis.

CONCLUSIONS

The overall aim of this article is to demonstrate that the coarse-grained model of ref 11 can help guide the design of a complex nanotechnological DNA system by providing significant insight into its operation. In particular, the model can be used to explore non-equilibrium effects that are central to the operation of synthetic molecular devices and also highlight the effects of DNA structure and mechanics on a system's kinetics.

To make the case for applying this computational methodology to guide the design of a wide range of nanotechnological DNA systems, we explored in detail the operation of the two-footed DNA walker introduced in ref 12. In particular, we have studied the processes by which the walker's feet rebind to the track, demonstrating that the walker's motion is governed by a subtle balance of kinetic and thermodynamic factors. To our knowledge, this is the first time a model of this detail has been used to predict behavior and suggest optimization strategies for a synthetic DNA system. Our principle findings are the following. (1) Applying a tension of approximately 15 pN to the track can help to bias the walker toward binding a raised foot immediately in front of the stationary foot (rather than immediately behind), without significantly changing the nature of the fully bound state. (2) The walker has a tendency to overstep on extended tracks, even when they are held under tension. (3) When in an overstepped state, the walker/track duplex has an exaggerated tendency to fray from its front edge if the track is held under tension, opening up a toehold for the fuel to displace the track and allow the system to recover. This extra fraying is not observed in the absence of tension. (4) The presence of remnants of nicked fuel can influence binding kinetics as both halves of the fuel are unlikely to detach before rebinding begins. We find that, neglecting any effects of the enzyme, displacement of the whole fuel by the track is somewhat faster (by a factor of $\sim$4) than spontaneous dissociation of one or other half of the fuel in our model, which is generally followed by displacement of the remaining fuel segment. The relative rates of displacement and spontaneous dissociation for real DNA are sensitive to a number of factors that are not fully described by the model, such as the effect of mismatches and the behavior of the enzyme. However, our results clearly suggest that rebinding prior to any spontaneous dissociation of the fuel should be a relevant process with the current design, reducing the efficiency of the walker. (5) In the case where one-half of the fuel detaches spontaneously, the behavior of the system is strongly dependent on which half remains. If the domain closest to the body of the walker (the proximal half) is still present, the intended binding to the site immediately in front of the stationary foot is suppressed, resulting in overstepping or binding behind the stationary foot. By contrast, if the domain furthest from the walker's body (the distal half) remains, the tension-induced bias for binding immediately in front of the stationary foot (rather than behind it) is preserved, and overstepping is also less significant.

These results suggest modifications to the design of the walker to improve its operation. Most obviously, it

would be desirable to reduce the tendency of the walker to overstep. Although fraying of the overstepped duplex will allow recovery, overstepping will result in a number of wasted cycles, reducing efficiency and speed. One approach would be to redesign the system so that the two feet are not identical. The track would then have two distinct competition domains and two distinct binding domains, and two fuel strands would be needed (one to lift each foot). Overstepping by a single site could then be essentially eliminated.

Second, it is desirable that the proximal half of the fuel should detach before the distal half detaches either spontaneously or through displacement by the track. Preferential detachment of the proximal half of the fuel could be achieved by making the nick site closer to the body of the walker or by including a higher proportion of weaker A-T base pairs in this section. Any tendency for the distal half of the fuel to be displaced by the track before the proximal half spontaneously detaches could also be suppressed by making the toehold for binding offered by the competition domain less effective. Several alternatives (including making the fuel longer, including a track/foot mismatch in the competition domain) are possible—the optimal choice will require further experimental investigation.

The majority of the results in this work depend on a combination of the physics of duplex formation and the structural and mechanical properties of single- and double-stranded DNA. These are features that the coarse-grained model has been shown to reproduce accurately.[11] For example, preferential binding to various sites results from the physical proximity of bases that can nucleate duplex formation, a result that should be robust to the approximations involved in the model, provided that DNA duplexes do indeed form by first nucleating a small number of base pairs. The most important unknown factor is that we cannot analyze the influence of the nicking enzyme on rebinding. Whatever its role, however, it seems likely that the proximal half of the raised fuel should be designed to dissociate before the distal half detaches or is displaced. Experimental studies into the mechanism by which the nicking enzyme operates may help to elucidate how relevant it is to this aspect of the design.

METHODS

We use two basic simulation techniques to study the model's representation of the walker. To sample equilibrium thermodynamics, we employ virtual move Monte Carlo (VMMC),[38,39] an efficient Monte Carlo algorithm which moves clusters of interacting particles. For kinetic results, we use the rigid-body Langevin dynamics (LD) algorithm of Davidchack *et al.*[40] Langevin algorithms reproduce the diffusive motion of particles and sample from the equilibrium ensemble. Many of the processes relevant to walker operation are difficult to sample due to high free-energy barriers between metastable states. To enhance equilibration of thermodynamic VMMC simulations, an artificial bias is used to flatten the free-energy landscape in a technique known as umbrella sampling.[41] Umbrella sampling, however, cannot be used to enhance the sampling of dynamical trajectories, as it produces biased dynamics. When brute force Langevin simulations are impractical, we use forward flux sampling[42,43] (FFS), a technique in which the flux from one metastable minimum to another is measured in stages. More details of all simulation techniques are provided in the Supporting Information.

Conflict of Interest: The authors declare no competing financial interest.

Acknowledgment. T.O. would like to acknowledge financial support from University College, Oxford, and thank R. Machinek for helpful discussions. This research was supported by EPSRC Grants EP/G037930/1 and EP/I001352/1. A.J.T. is supported by a Royal Society Wolfson Research Merit Award.

Supporting Information Available: Outline of the generic algorithms (VMMC, LD, umbrella sampling, FFS) used in this work, along with specifics relating to implementation. We also describe a simple rate model used to interpret our data on the displacement of nicked fuel by the track. This material is available free of charge *via* the Internet at http://pubs.acs.org.

REFERENCES AND NOTES

1. Seeman, N. C. Nucleic Acid Junctions and Lattices. *J. Theor. Biol.* **1982**, *99*, 237–247.
2. Watson, J. D.; Crick, F. H. C. Molecular Structure of Nucleic Acids. *Nature* **1953**, *171*, 737–738.
3. Saenger, W. *Principles of Nucleic Acid Structure*; Springer-Verlag: New York, 1984.
4. Pinheiro, A. V.; Han, D.; Shih, W. M.; Yan, H. Challenges and Opportunities for Structural DNA Nanotechnology. *Nat. Nanotechnol.* **2011**, *6*, 763–772.
5. Bath, J.; Turberfield, A. J. DNA Nanomachines. *Nat. Nanotechnol.* **2007**, *2*, 275–284.
6. Masoud, R.; Tsukanov, R.; Tomov, T. E.; Plavner, N.; Liber, M.; Nir, E. Studying the Structural Dynamics of Bipedal DNA Motors with Single-Molecule Fluorescence Spectroscopy. *ACS Nano* **2012**, *6*, 6272–6283.
7. SantaLucia, J., Jr.; Hicks, D. The Thermodynamics of DNA Structural Motifs. *Annu. Rev. Biophys. Biomol. Struct.* **2004**, *33*, 415–440.
8. Dirks, R. M.; Bois, J. S.; Schaeffer, J. M.; Winfree, E.; Pierce, N. A. Thermodynamic Analysis of Interacting Nucleic Acid Strands. *SIAM Rev.* **2007**, *29*, 65–88.
9. Liedl, T.; Högberg, B.; Tytell, J.; Ingbe, D. E.; Shih, W. M. Self-Assembly of Three-Dimensional Prestressed Tensegrity Structures from DNA. *Nat. Nanotechnol.* **2010**, *5*, 520–524.
10. Lavery, R.; Zakrzewska, K.; Beveridge, D.; Bishop, T. C.; Case, D. A.; Cheatham, T., III; Dixit, S.; Jayaram, B.; Lankas, F.; Laughton, C.; *et al.* A Systematic Molecular Dynamics Study of Nearest-Neighbor Effects on Base Pair and Base Pair Step Conformations and Fluctuations in B-DNA. *Nucleic Acids Res.* **2010**, *38*, 299–313.
11. Ouldridge, T. E.; Louis, A. A.; Doye, J. P. K. Structural, Mechanical and Thermodynamic Properties of a Coarse-Grained Model of DNA. *J. Chem. Phys.* **2011**, *134*, 085101.
12. Bath, J.; Green, S. J.; Allan, K. E.; Turberfield, A. J. Mechanism for a Directional, Processive and Reversible DNA Motor. *Small* **2009**, *5*, 1513–1516.
13. Yurke, B.; Mills, A. Using DNA to Power Nanostructures. In *Genetic Programming and Evolvable Machines*; Kluwer: Dordrecht, The Netherlands, 2003; Vol. 4, pp 111–122.
14. Yurke, B.; Turberfield, A. J.; Mills, A. P.; Simmel, F. C.; Neumann, J. A DNA-Fueled Molecular Machine Made of DNA. *Nature* **2000**, *406*, 605–608.

15. Goodman, R. P.; Heilemann, M.; Doose, S.; Erben, C. M.; Kapanidis, A. N.; Turberfield, A. J. Reconfigurable, Braced, Three-Dimensional DNA Nanostructures. *Nat. Nanotechnol.* **2008**, *3*, 93–96.
16. Andersen, E. S.; Dong, M.; Nielsen, M. M.; Jahn, K.; Subramani, R.; Mamdouh, W.; Golas, M. M.; Sander, B.; Stark, H.; Oliveira, C. L. P.; *et al.* Self-Assembly of a Nanoscale DNA Box with a Controllable Lid. *Nature* **2009**, *459*, 73–76.
17. Lo, P. K.; Karam, P.; Aldaye, F.; McLaughlin, C. K.; Hamblin, G.; Cosa, G.; Sleiman, H. F. Loading and Selective Release of Cargo in DNA Nanotubes with Longitudinal Variation. *Nat. Chem.* **2010**, *2*, 319–328.
18. Han, D.; Pal, S.; Liu, Y.; Yan, H. Folding and Cutting DNA into Reconfigurable Topological Nanostructures. *Nat. Nanotechnol.* **2010**, *5*, 712–717.
19. Sherman, W. B.; Seeman, N. C. A Precisely Controlled DNA Biped Walking Device. *Nano Lett.* **2004**, *4*, 1203–1207.
20. Shin, J.-S.; Pierce, N. A. A Synthetic DNA Walker for Molecular Transport. *J. Am. Chem. Soc.* **2004**, *126*, 10834–-10835.
21. Bath, J.; Green, S. J.; Turberfield, A. J. A Free-Running DNA Motor Powered by a Nicking Enzyme. *Angew. Chem., Int. Ed.* **2005**, *117*, 4432–4435.
22. Tian, Y.; He, Y.; Chen, Y.; Yin, P.; Mao, C. A DNAzyme That Walks Processively and Autonomously along a One-Dimensional Track. *Angew. Chem., Int. Ed.* **2005**, *44*, 4355–4358.
23. Wickham, S. F. J.; Endo, M.; Katsuda, Y.; Hidaka, K.; Bath, J.; Sugiyama, H.; Turberfield, A. J. Direct Observation of Stepwise Movement of a Synthetic Molecular Transporter. *Nat. Nanotechnol.* **2011**, *6*, 166–169.
24. Turberfield, A. J.; Mitchell, J. C.; Yurke, B.; Mills, A. P.; Blakey, M. I.; Simmel, F. C. DNA Fuel for Free-Running Nanomachines. *Phys. Rev. Lett.* **2003**, *90*, 118102–118105.
25. Omabegho, T.; Sha, R.; Seeman, N. C. A Bipedal DNA Brownian Motor with Coordinated Legs. *Science* **2009**, *324*, 67–71.
26. Green, S. J.; Bath, J.; Turberfield, A. J. Coordinated Chemomechanical Cycles: A Mechanism for Autonomous Molecular Motion. *Phys. Rev. Lett.* **2008**, *101*, 238101.
27. Venkataraman, S.; Dirks, R. M.; Rothemund, P. W. K.; Winfree, E.; Pierce, N. A. An Autonomous Polymerization Motor Powered by DNA Hybridization. *Nat. Nanotechnol.* **2007**, *2*, 490–494.
28. Muscat, R. A.; Bath, J.; Turberfield, A. J. A Programmable Molecular Robot. *Nano Lett.* **2011**, *11*, 982–987.
29. He, Y.; Liu, D. R. Autonomous Multistep Organic Synthesis in a Single Isothermal Solution Mediated by a DNA Walker. *Nat. Nanotechnol.* **2010**, *5*, 778–782.
30. Gu, H.; Chao, J.; Xiao, S.; Seeman, N. C. A Proximity-Based Programmable DNA Nanoscale Assembly Line. *Nature* **2010**, *465*, 202–205.
31. Heiter, D. F.; Lunnen, K. D.; Wilson, G. G. Site-Specific DNA-Nicking Mutants of the Heterodimeric Restriction Endonuclease R.BbvCI. *J. Mol. Biol.* **2005**, *348*, 631–640.
32. Ouldridge, T. E. Coarse-Grained Modelling of DNA and DNA Nanotechnology. Ph.D. Thesis, University of Oxford, 2011; http://tinyurl.com/7ycbx7c.
33. Ouldridge, T. E.; Louis, A. A.; Doye, J. P. K. DNA Nanotweezers Studied with a Coarse-Grained Model of DNA. *Phys. Rev. Lett.* **2010**, *104*, 178101.
34. Romano, F.; Chakraborty, D.; Doye, J. P. K.; Ouldridge, T. E.; Louis, A. A. Coarse-Grained Simulations of DNA Overstretching. *J. Chem. Phys.* **2013**, *138*, 085101.
35. Matek, C.; Ouldridge, T. E.; Levy, A.; Doye, J. P. K.; Louis, A. A. DNA Cruciform Arms Nucleate Through a Correlated but Asynchronous Cooperative Mechanism. *J. Phys. Chem. B* **2012**, *116*, 11616–11625.
36. Michele, C. D.; Rovigatti, L.; Bellini, T.; Sciortino, F. Self-Assembly of Short DNA Duplexes: From a Coarse-Grained Model to Experiments through a Theoretical Link. *Soft Matter* **2012**, *8*, 8388–8398.
37. SantaLucia, J., Jr. A Unified View of Polymer, Dumbbell, and Oligonucleotide DNA Nearest-Neighbor Thermodynamics. *Proc. Natl. Acad. Sci. U.S.A.* **1998**, *17*, 1460–1465.
38. Whitelam, S.; Geissler, P. L. Avoiding Unphysical Kinetic Traps in Monte Carlo Simulations of Strongly Attractive Particles. *J. Chem. Phys.* **2007**, *127*, 154101.
39. Whitelam, S.; Feng, E. H.; Hagan, M. F.; Geissler, P. L. The Role of Collective Motion in Examples of Coarsening and Self-Assembly. *Soft Matter* **2009**, *5*, 1251–1262.
40. Davidchack, R. L.; Handel, R.; Tretyakov, M. V. Langevin Thermostat for Rigid Body Dynamics. *J. Chem. Phys.* **2009**, *130*, 234101.
41. Torrie, G. M.; Valleau, J. P. Nonphysical Sampling Distributions in Monte Carlo Free-Energy Estimation: Umbrella Sampling. *J. Comput. Phys.* **1977**, *23*, 187–199.
42. Allen, R. J.; Warren, P. B.; ten Wolde, P. R. Sampling Rare Switching Events in Biochemical Networks. *Phys. Rev. Lett.* **2005**, *94*, 018104.
43. Allen, R. J.; Valeriani, C.; ten Wolde, P. R. Forward Flux Sampling for Rare Event Simulations. *J. Phys.: Condens. Matter* **2009**, *21*, 463102.
44. Murtola, T.; Bunkwer, A.; Vattulainen, I.; Deserno, M. Multiscale Modeling of Emergent Materials: Biological and Soft Matter. *Phys. Chem. Chem. Phys.* **2009**, *11*, 1869–1892.
45. Mills, J. B.; Vacano, E.; Hagerman, P. J. Flexibility of Single-Stranded DNA: Use of Gapped Duplex Helices To Determine the Persistence Lengths of Poly(dT) and Poly(dA). *J. Mol. Biol.* **1999**, *285*, 245–257.
46. Huguet, J. M.; Bizarro, C. V.; Forns, N.; Smith, S. B.; Bustamante, C.; Ritort, F. Single-Molecule Derivation of Salt Dependent Base-Pair Free Energies in DNA. *Proc. Natl. Acad. Sci. U.S.A.* **2010**, *107*, 15431–15436.
47. Smith, S. B.; Cui, Y.; Bustamante, C. Overstretching B-DNA: The Elastic Response of Individual Double-Stranded and Single-Stranded DNA Molecules. *Science* **1996**, *271*, 795–799.